Block Matrix Preconditioner for the Coupled Volume-Surface Integral Equation

Shifei Tao

Department of Communication Engineering
Nanjing University of Science and Technology, Nanjing 210094, China
taoshifei71@163.com

Abstract ─ A Block Matrix Preconditioner (BMP) for Volume and Surface Electric Field Integral Equations (V-EFIE and S-EFIE) for the analysis of electromagnetic scattering problems is presented. The V-EFIE operator is well-posed while the S-EFIE operator is ill-posed, so for the coupled V-EFIE and S-EFIE system, it is ill-conditioned. Therefore, the solution time is very long if the iterative solution is applied to solve the system equations. The proposed scheme constructs a sparse matrix version of each block matrix, which is followed by the inversion of the resultant block sparse matrix using incomplete factorization. The proposed scheme enables the efficient electromagnetic analysis for the composite structures. Several numerical examples are proposed to demonstrate the efficiency of the scheme.

Index Terms ─ Block matrix preconditioner, coupled volume-surface integral equation and iterative solution.

I. INTRODUCTION

Numerical analysis of electromagnetic scattering from composite structures comprising PEC and dielectric materials has been attracting researchers due to their kinds of useful applications, such as PEC targets coated dielectric radar absorbing materials, microstrip structures on finite substrates, etc. The integral equation methods using the Method of Moments (MoM) [1] have been among the most popular methods for their generality. The coupled Volume and Surface Integral Equations (VSIE) [2-3] formulation is a typical method for these problems. In this approach, the Volume Electric Field Integral Equation (V-EFIE) is applied in the dielectric region, while the Surface Electric Field Integral Equation (S-EFIE) is applied on the PEC surface. The V-EFIE operators are bounded and well-posed, even though applied to densely discretized cells [4]; while S-EFIE operators are often ill-posed, especially for the dense surface discretization [5-6]. As a result, the coupled V-EFIE and S-EFIE are ill-conditioned, so the iterative solution becomes so expensive. For some special problems, we can't even get the expected results. In recent years, some technologies are proposed to reduce the iterations steps or make the solving process easier [7-14].

The Block Matrix Preconditioner (BMP) originally proposed by the FEM community [15-16], is applied to address the convergence problem by the MoM for PEC [17] and penetrable objects [18]. In this paper, the similar procedure is applied for the coupled volume-surface integral equations system. To compute the BMP efficiently, we first create a sparse matrix from each block matrix by eliminating the small terms in the matrix entries and the inversion of the constructed sparse matrix is approximated using incomplete factorization. Finally, the BMP constructed using the proposed method is compared with the Incomplete LU Threshold Pivoting (ILUTP) preconditioner [19] to demonstrate their performance in terms of memory and computation time.

This paper is organized as follows. The basic theory and formulations about the coupled VSIE and the block matrix preconditioner are given in section II. Numerical results obtained with the scheme described in this paper are shown and analyzed in section III and the remarks are included in section IV.

Submitted On: February 26, 2013
Accepted On: January 27, 2014

II. THEROY AND FORMULATIONS

A. Coupled volume-surface electric field integral equations

Consider a plane wave incident upon an arbitrarily shaped composite structure comprising PEC surfaces S and dielectric volumes V in free space. It is assumed that the permeability is all μ_0 for all of space, the permittivity are $\hat{\varepsilon}$ and ε_0 for the volumes V and free space, respectively. The dielectric volumes V are replaced by volume currents $\vec{J}_V$ and the PEC surfaces S are replaced by surface currents $\vec{J}_S$. In this paper, time dependence $e^{j\omega t}$ is assumed and suppressed. Based on the boundary conditions of the total electric field, we can get the coupled volume-surface electric field integral equations as:

$$\vec{E}^{inc} = \frac{\vec{D}(\vec{r})}{\hat{\varepsilon}(\vec{r})} + j\omega\vec{A}_V(\vec{r}) + \nabla\Phi_V(\vec{r}) + j\omega\vec{A}_S(\vec{r}) + \nabla\Phi_S(\vec{r}) \qquad \vec{r}\in V, \tag{1}$$

$$\vec{E}^{i}_{\tan} = [\, j\omega\vec{A}_V(\vec{r}) + \nabla\Phi_V(\vec{r}) + j\omega\vec{A}_S(\vec{r}) + \nabla\Phi_S(\vec{r})]_{\tan} \qquad \vec{r}\in S. \tag{2}$$

Here, $\vec{E}^{inc}$ is the incident electric field, "tan" represents the tangential to the PEC surface. $\vec{D}$ is the electric flux densities and $\vec{D}(\vec{r}) = \vec{J}_V(\vec{r}) \big/ \left(j\omega\hat{\chi}(\vec{r}) \right)$, $\hat{\chi}$ is the contrast parameter and $\hat{\chi} = \left(\hat{\varepsilon}(\vec{r}) - \varepsilon_0\right) \big/ \hat{\varepsilon}(\vec{r})$. $\vec{A}_V(\vec{r})$, $\Phi_V(\vec{r})$, $\vec{A}_S(\vec{r})$ and $\Phi_S(\vec{r})$ are the vector magnetic potentials and scalar electric potentials produced by the surface and volume currents, respectively.

The electric flux densities $\vec{D}$ and surface currents $\vec{J}_S$ are chosen as the unknowns in this paper. The volumes V and surfaces S are meshed by tetrahedrons and triangles. The SWG and RWG basis function are applied to represent electric flux densities $\vec{D}$ and surface currents $\vec{J}_S$, respectively. After the Galerkin's testing, equations (1) and (2) are converted to matrix equations:

$$\begin{bmatrix} Z^{DD} & Z^{DM} \\ Z^{MD} & Z^{MM} \end{bmatrix} \begin{bmatrix} I^D \\ I^M \end{bmatrix} = \begin{bmatrix} V^D \\ V^M \end{bmatrix}. \tag{3}$$

The impedance matrix $[Z]$ consists of four parts: $[Z^{DD}]$, $[Z^{DM}]$, $[Z^{MD}]$ and $[Z^{MM}]$, which account for volume basis test volume basis, volume basis test surface basis, surface basis test volume basis and surface basis test surface basis, respectively. $[I]$ and $[V]$ are the vectors of expansion coefficients and tested incident filed. The detail forms of matrix equations are given as follows:

$$\int_V \vec{f}_m^V(\vec{r}) \cdot \vec{E}^i d\vec{r} = \underbrace{\int_{V_m} \vec{f}_m^V(\vec{r}) \cdot \frac{\vec{D}(\vec{r}\,')}{\hat{\varepsilon}(\vec{r}\,')} d\vec{r} + j\omega \int_{V_m} \vec{f}_m^V(\vec{r}) \cdot \vec{A}_V(\vec{r}\,') d\vec{r} - \int_{V_m} (\nabla \cdot \vec{f}_m^V(\vec{r})) \Phi_V(\vec{r}\,') d\vec{r} + \int_{\Omega_m} (\vec{n} \cdot \vec{f}_m^V(\vec{r})) \Phi_V(\vec{r}\,') d\vec{r}}_{Z^{DD}},$$

$$\underbrace{+ j\omega \int_{V_m} \vec{f}_m^V(\vec{r}) \cdot \vec{A}_S(\vec{r}\,') d\vec{r} - \int_{V_m} (\nabla \cdot \vec{f}_m^V(\vec{r})) \Phi_S(\vec{r}\,') d\vec{r} + \int_{\Omega_m} (\vec{n} \cdot \vec{f}_m^V(\vec{r})) \Phi_S(\vec{r}\,') d\vec{r}}_{Z^{MD}} \tag{4}$$

$$\int_S \vec{f}_m^S(\vec{r}) \cdot \vec{E}^i d\vec{r} = \underbrace{j\omega \int_{S_m} \vec{f}_m^S(\vec{r}) \cdot \vec{A}_V(\vec{r}\,') d\vec{r} - \int_{S_m} (\nabla \cdot \vec{f}_m^S(\vec{r})) \Phi_V(\vec{r}\,') d\vec{r}}_{Z^{DM}},$$

$$\underbrace{+ j\omega \int_{S_m} \vec{f}_m^S(\vec{r}) \cdot \vec{A}_S(\vec{r}\,') d\vec{r} - \int_{S_m} (\nabla \cdot \vec{f}_m^S(\vec{r})) \Phi_S(\vec{r}\,') d\vec{r}}_{Z^{MM}} \tag{5}$$

Green's function used in the integral operators is the free-space Green's function in the VSIE approach. Hence, the MLFMA can be easily applied to reduce the computational complexity and memory requirement [20]. The basic idea of the MLFMA is to convert the interaction of element-to-element to the interaction of group-to-group. Here, a group includes the elements residing in a spatial box. The mathematical foundation of the MLFMA is the addition theorem for the scalar Green's function in free space. Using the MLFMA, the matrix-vector product can be

split into near interaction part and far interaction part. The calculation of matrix elements in the near interaction part remains the same as in the MoM procedure. However, those elements in the far interaction part are not explicitly computed and stored. When the MLFMA is implemented in VSIE, we can obtain:

$$\frac{j\omega\mu_0}{4\pi}\int_{V_m}\vec{f}_m^{\,V}(\vec{r})\cdot\int_{V_n}\bar{\mathbf{G}}(\vec{r},\vec{r}\,')\vec{J}_V(\vec{r}\,')d\vec{r}\,'d\vec{r} = R_{mp}^V(\hat{k})\Gamma_{pq}(\hat{k},\hat{r}_{pq})F_{qn}^V(\hat{k}), \quad (6a)$$

$$\frac{j\omega\mu_0}{4\pi}\int_{S_m}\vec{f}_m^{\,S}(\vec{r})\cdot\int_{S_n}\bar{\mathbf{G}}(\vec{r},\vec{r}\,')\vec{J}_S(\vec{r}\,')d\vec{r}\,'d\vec{r} = R_{mp}^S(\hat{k})\Gamma_{pq}(\hat{k},\hat{r}_{pq})F_{qn}^S(\hat{k}), \quad (6b)$$

where $\bar{\mathbf{G}}(\vec{r},\vec{r}\,')$ is the dyadic Green's function, $R_{mp}^V(k)$ and $R_{mp}^S(k)$ denote the distribution factor, $\Gamma_{pq}(k,\hat{r}_{pq})$ denotes the translator factor and $F_{qn}^V(k)$ and $F_{qn}^S(k)$ denote the aggregation distribution factor. They are given by the following equation:

$$\bar{\mathbf{G}}(\vec{r},\vec{r}\,') = \left[\bar{\mathbf{I}}+\frac{1}{k^2}\nabla\nabla\right]\frac{e^{-jk|\vec{r}-\vec{r}\,'|}}{|\vec{r}-\vec{r}\,'|}, \quad (7a)$$

$$F_{qn}^V(k) = \int_{V_n}(\bar{\mathbf{I}}-kk)\,j\omega K_n\vec{f}_n^{\,V}(\vec{r}\,')e^{-j\mathbf{k}\cdot\mathbf{r}_{qn}}d\vec{r}\,', \quad (7b)$$

$$R_{mp}^V(k) = \int_{V_m}(\bar{\mathbf{I}}-kk)\,\vec{f}_m^{\,V}(\vec{r})e^{-j\mathbf{k}\cdot\mathbf{r}_{mp}}d\vec{r}, \quad (7c)$$

$$\Gamma_{pq}(k,\hat{r}_{pq}) = \frac{k\omega\mu_0}{(4\pi)^2}\alpha_{pq}(\hat{r}_{pq}\cdot k), \quad (7d)$$

$$F_{qn}^S(k) = \int_{V_n}(\bar{\mathbf{I}}-kk)\,\vec{f}_n^{\,S}(\vec{r}\,')e^{-j\mathbf{k}\cdot\mathbf{r}_{qn}}d\vec{r}\,', \quad (7e)$$

$$R_{mp}^S(k) = \int_{V_m}(\bar{\mathbf{I}}-kk)\,\vec{f}_m^{\,S}(\vec{r})e^{-j\mathbf{k}\cdot\mathbf{r}_{mp}}d\vec{r}. \quad (7f)$$

B. Blocker matrix preconditioner

An effective preconditioner can be incorporated into iterative methods to improve the convergence rate. The preconditioned matrix equation can be solved as follows:

$$M^{-1}ZI = M^{-1}V, \quad (8)$$

where M is the precondition matrix, which should be a nonsingular matrix with the same order of Z. In general, the precondition matrix M should be chosen to make sure that the condition number of the preconditioned matrix $M^{-1}Z$ is less than that of matrix Z, which can reduce the computation time for iterative methods to solve the matrix equation. An improper choice for M would worsen the preconditioned system.

In equation (3), because matrices Z^{DD}, Z^{MD}, Z^{DM} and Z^{MM} in the conventional MoM are all dense matrices, sparse versions of these matrices should be gotten when computing the inversion of a precondition matrix M^{-1} [21]. Therefore, we should construct the sparse forms of these matrices. Firstly, the elements of the impedance matrix are normalized row by row, which makes the amplitude of the biggest element of each row to be 1, so the other elements are all less than 1. Then a threshold $\delta\in(0,1)$ is set during the removing procedure, which can control the sparseness of matrix. If the normalized elements are less than δ, the elements should be abandoned. The smaller δ is, the sparser the impedance matrix is. To control the account of saved elements of each row, a parameter $\mathrm{K}_{\max}$ is chosen. If the number of saved elements of one row is greater than $\mathrm{K}_{\max}$, we just need to keep the $\mathrm{K}_{\max}$ biggest elements. If the dimension of the impedance matrix is N, then total number of elements in the sparse matrix is less or equal $\mathrm{K}_{\max}$ *N. The introducing of $\mathrm{K}_{\max}$ is very helpful for allocating the array to store the preconditioner matrix during the coding procedure.

For the amplitudes of elements in the four parts of coupled VSIE impedance matrix vary a lot, to ensure the strong coupling elements of each part are included in the sparse matrix, the procedure of constructing sparse matrices for the Z^{DD}, Z^{MD}, Z^{DM} and Z^{MM} are implemented, respectively.

Once the block sparse matrices were constructed, the BMP can be computed using Gaussian elimination of the block matrix system. The 2×2 block matrix can be decomposed into matrix product:

$$Z_{\text{near}} \approx \begin{bmatrix} Z_{\text{sparse}}^{DD} & Z_{\text{sparse}}^{DM} \\ Z_{\text{sparse}}^{MD} & Z_{\text{sparse}}^{MM} \end{bmatrix} = \begin{bmatrix} I^{DD} & 0 \\ Z_{\text{sparse}}^{MD}\left(Z_{\text{sparse}}^{DD}\right)^{-1} & I^{MM} \end{bmatrix} \begin{bmatrix} Z_{\text{sparse}}^{DD} & 0 \\ 0 & Z_{\text{sparse}}^{MM} - Z_{\text{sparse}}^{MD}\left(Z_{\text{sparse}}^{DD}\right)^{-1} Z_{\text{sparse}}^{DM} \end{bmatrix} \begin{bmatrix} I^{DD} & \left(Z_{\text{sparse}}^{DD}\right)^{-1} Z_{\text{sparse}}^{DM} \\ 0 & I^{MM} \end{bmatrix} \tag{9}$$

and its inverse can be found as follows:

$$\left(Z_{\text{near}}\right)^{-1} \approx \begin{bmatrix} I^{DD} & -\left(Z_{\text{sparse}}^{DD}\right)^{-1} Z_{\text{sparse}}^{DM} \\ 0 & I^{MM} \end{bmatrix} \begin{bmatrix} \left(Z_{\text{sparse}}^{DD}\right)^{-1} & 0 \\ 0 & \left(Z_{\text{sparse}}^{MM} - Z_{\text{sparse}}^{MD}\left(Z_{\text{sparse}}^{DD}\right)^{-1} Z_{\text{sparse}}^{DM}\right)^{-1} \end{bmatrix} \begin{bmatrix} I^{DD} & 0 \\ -Z_{\text{sparse}}^{MD}\left(Z_{\text{sparse}}^{DD}\right)^{-1} & I^{MM} \end{bmatrix} \tag{10}$$

where I^{DD} and I^{MM} are the identity matrices of size $N^D \times N^D$ and $N^M \times N^M$; N^D and N^M indicate the number of SWG basis functions and RWG basis functions, respectively.

The block matrix in equation (10) involves inversion of both the first block Z_{sparse}^{DD} and the Schur complement, which can be represented as follows: $S = Z_{\text{sparse}}^{MM} - Z_{\text{sparse}}^{MD}\left(Z_{\text{sparse}}^{DD}\right)^{-1} Z_{\text{sparse}}^{DM}$. For the time for computing the coupling of $Z_{\text{sparse}}^{MD}\left(Z_{\text{sparse}}^{DD}\right)^{-1} Z_{\text{sparse}}^{DM}$ is very consuming, the Schur complement S has been approximated as the inversion of Z_{sparse}^{MM} during the construction of preconditioner in this paper, also the similar treatment has been taken in [18]. Finally, the proposed BMP M^{-1} can be determined as follows:

$$M^{-1} = \begin{bmatrix} I^{DD} & -\left(Z_{\text{sparse}}^{DD}\right)^{-1} Z_{\text{sparse}}^{DM} \\ 0 & I^{MM} \end{bmatrix} \begin{bmatrix} \left(Z_{\text{sparse}}^{DD}\right)^{-1} & 0 \\ 0 & \left(Z_{\text{sparse}}^{MM}\right)^{-1} \end{bmatrix} \begin{bmatrix} I^{DD} & 0 \\ -Z_{\text{sparse}}^{MD}\left(Z_{\text{sparse}}^{DD}\right)^{-1} & I^{MM} \end{bmatrix}. \tag{11}$$

This preconditioner can be applied at each iteration in iterative methods via matrix multiplication. Because the BMP requires the inversion of each block matrix Z_{sparse}^{DD} and Z_{sparse}^{MM} separately, different dropping parameters can be applied to the approximate inverse methods such as Incomplete LU (ILU) decomposition and the Sparse Approximate Inverse method (SAI). In this paper, the ILU decomposition preconditioner is applied, which is widely used and available in several solver packages. There are two popular drop strategies for ILU factorization; the level based drop strategy and the threshold based drop strategy, the former is denoted ILU(p), where $p \geq 0$ is an integer denoted as the level of fill-in and the latter is ILUTP. For the ILUTP preconditioner is highly stable and has a fast convergence rate performance and it is chosen as the approximate inverse methods in this paper.

III. NUMRICAL RESULTS

In this section, three numerical examples are presented for the accuracy and efficiency of the approach in this paper. The iteration process is terminated when the 2-norm residual error is reduced by 1×10^{-3} and the restarted GMRES (30) is selected as the iterative method, where 30 is the dimension size of Krylov subspace for GMRES. Zero vector is taken as initial approximate solution for all examples. During the construction of sparse forms of preconditioner matrices, the choice for δ and $\mathrm{K}_{\max}$ is very important. For δ and $\mathrm{K}_{\max}$ is set as 0.01 and 200, respectively. The larger $\mathrm{K}_{\max}$ (the smaller δ) is, the less the number of steps needed for iteration solution, but it will cost more time and memory requirement for constructing

precondition matrix. Actually, there is a balance between the number of steps for iteration solution and time and memory requirement for constructing precondition matrix. If the computational platform is powerful (huge memory and large number of CPUs) and we just care for the fast convergence of the solution, K_{max} can be chosen as large as possible. In this paper, all the numerical examples are performed on the PC with an Intel Core 2 (3 GHz CPU) and 3.2 GB RAM, so δ and K_{max} is set as 0.01 and 200, respectively; which are suitable numbers for the computational platform used in this paper. For electric small objects, the K_{max} can be set as largely as possible, because the time and memory requirement needed for constructing precondition matrix won't be an obstacle. For electric large objects, the choice for K_{max} mainly depends on the computational platform.

For the first example, we consider a conducting sphere coated by dielectric material. The permittivity of dielectric material is $\varepsilon_r=2$.The radii of the inner and outer surface of the dielectric shell are $0.2\lambda_0$ and $0.25\lambda_0$, respectively. λ_0 is the wavelength in the free space. The surface of the conducting sphere is discretized into 480 triangles and the volume of the dielectric shell into 1674 tetrahedrons, yielding a total number of 4627 unknowns including 720 RWG basis and 3907 SWG basis. Figure 1 shows the bistatic Radar Cross-Section (RCS) for a normally incident plane wave on the sphere. It is observed that the results obtained by the ILUTP preconditioned and BMP preconditioned VSIE are all in excellent agreement with Mie series solution, which are analytical results. Figure 2 shows the convergence history when the BMP and the ILUTP preconditioner are used to solve the coupled VSIE system resulting from the use of the MoM.

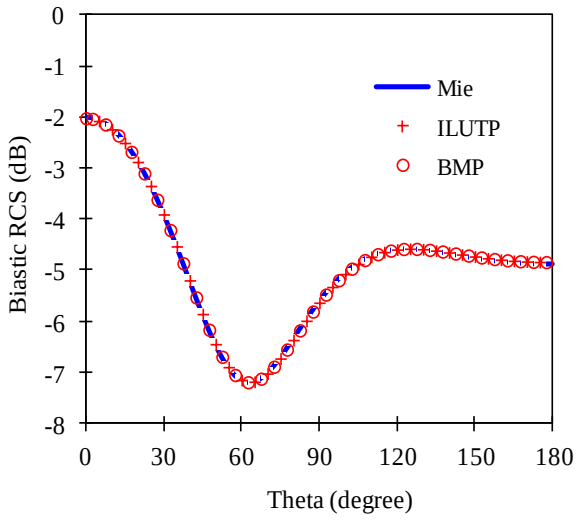

Fig. 1. The bistatic RCS (Phi=0) of a coated sphere with inner and outer radii are $0.2\lambda_0$ and $0.25\lambda_0$, $\varepsilon_r=2$.

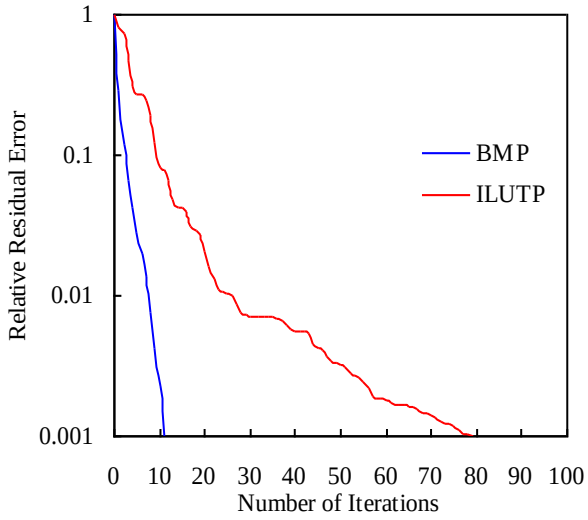

Fig. 2. The convergence history of the coated sphere.

The second example is a disk-cone structure [22], shown in the inset of Fig. 3. The dielectric

cone (ε_r=2) has a radius of $1.2\lambda_0$ and a height of $0.6\lambda_0$. The disk also has a radius of $1.2\lambda_0$. The number of the total unknowns is 13131, including 658 RWG basis and 12473 SWG basis. Figure 4 shows the convergence history when the BMP and the ILUTP preconditioner are used to solve thecoupled VSIE system resulting from the use of the FMM.

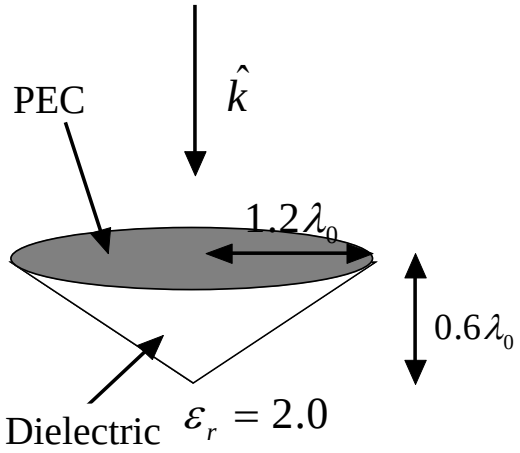

Fig. 3. The geometry of a disk-cone structure.

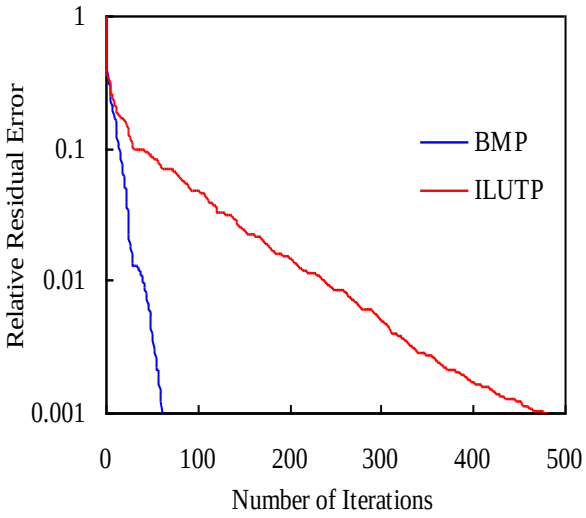

Fig. 4. The convergence history of the coated sphere.

Table 1 summarizes the computational demands of the ILUTP and the BMP for the two objects. In the second column, the number of RWG basis functions and SWG basis functions are included in parenthesis. As shown in Table 1, both the required construction time and the solution time of the BMP are considerably less than those of the ILUTP. Moreover, the BMP requires less memory storage than the ILUTP.

Table 1: The computational demands of the ILUTP and BMP for the two objects

	Unknowns (SWG, RWG)	Preconditioner	Construction Memory (MB)	Construction Time (S)	Steps of Iteration	Solutionl Time (S)
Coated sphere	4627 (3907, 720)	ILUTP	7.4	28	79	3.87
		BMP	6.1	21	11	0.76
Disk-cone	13131 (12473, 658)	ILUTP	23	215	480	126.8
		BMP	20	155	61	25.2

Next, we consider a Frequency-Selective Surface (FSS) structure with 64 (8×8) printed square-ring elements, as shown in Fig. 5. The size of the square ring is $D_1 = 5mm$ and $D_2 = 4mm$, the period is $6mm \times 6mm$, the thickness of the dielectric substrate is $0.5mm$ and relative permittivity is ε_r=3. The surface of the square-ring patches is discretized into 3072 inner lines and the volume of the dielectric into 60462 triangles, yielding a total number of 63534 unknowns for the FSS structure. Figure 6 gives the transmission coefficients of the FSS structure in the frequency band of 10 to 20 GHz, the plane wave incident upon the FSS normally is considered. For comparison, the results computed by the commercial software Designer are also shown in Fig. 6. Figure 7 shows the convergence history when the BMP and the ILUTP preconditioner are used to solve the coupled VSIE system resulting from the use of the FMM. It can be found out that the ILUTP preconditioned VSIE system cannot achieve the demanded iteration accuracy (1×10^{-3}) within 4000 steps during the resonant frequency band (13 GHz-18 GHz), while the BMP preconditioned VSIE system can still

work. Table 2 summarizes the computational demands of iteration procedure for the ILUTP and the BMP of the FSS structure.

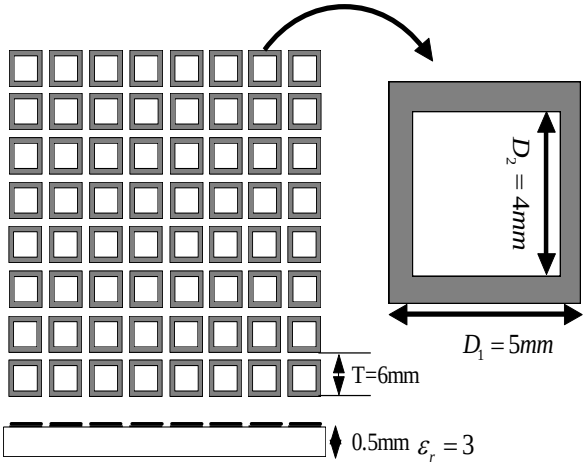

Fig. 5. The geometry of a FSS structure with 64 (8×8) printed square-ring elements.

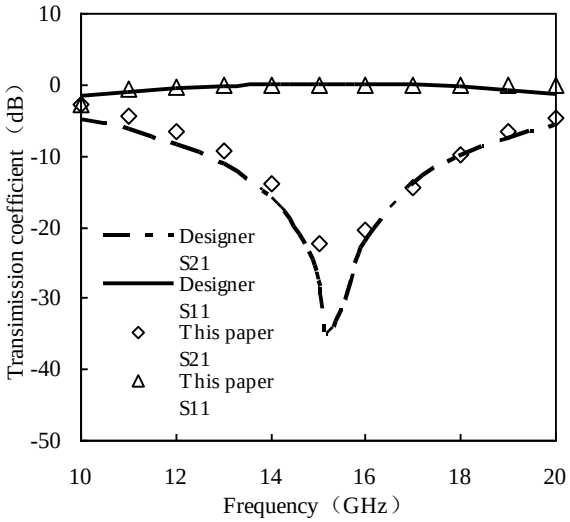

Fig. 6. Comparisons of transmission coefficients for the FSS structure between the results computed by Designer and by the proposed method in this paper.

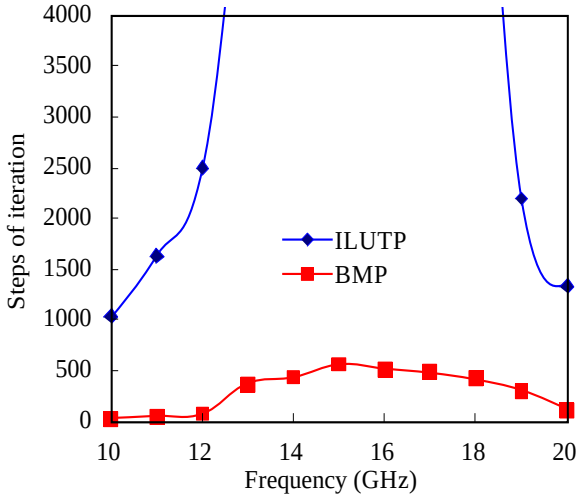

Fig. 7. The convergence history of the FSS structure.

Table 2: The iteration steps and solution time of the ILUTP and BMP for the FSS structure

Frequency (GHz)	Preconditioner	Steps of Iteration	Solution Time (S)
10	ILUTP	1036	257
	BMP	30	25
11	ILUTP	1631	424
	BMP	51	42
12	ILUTP	2499	1786
	BMP	77	63
13	ILUTP	>4000	-
	BMP	364	296
14	ILUTP	>4000	-
	BMP	436	352
15	ILUTP	>4000	-
	BMP	563	458
16	ILUTP	>4000	-
	BMP	512	413
17	ILUTP	>4000	-
	BMP	486	391
18	ILUTP	>4000	-
	BMP	421	332
19	ILUTP	2194	610
	BMP	302	239
20	ILUTP	1330	342
	BMP	112	90

IV. CONCLUSION

In this paper, a well conditioned coupled volume and surface electric field integral equations based on block matrix preconditioner combined with MLFMM is presented. The numerical results obtained by this scheme verified the accuracy and efficiency. Compared with the traditional ILUP preconditioner, the BMP preconditioner needs less iteration steps to achieve the expected precision and also shows a better performance in terms of construction time and memory usage.

REFERENCES

[1] R. F. Harrington, "Field computation by moment methods," *Krieger Publishing Company*, Florida, 1983.

[2] C. C. Lu and W. C. Chew, "A coupled surface-volume integral equation approach for the calculation of electromagnetic scattering from composite metallic and material targets," *IEEE Transactions on Antennas Propagation*, vol. 48, no. 12, pp. 1866-1868, December 2000.

[3] X. C. Nie, N. Yuan, L. W. Li, Y. B. Gan, and T. S. Yeo, "A fast volume-surface integral equation solver for scattering from composite conducting-dielectric objects," *IEEE Transactions on Antennas Propagation*, vol. 53, no. 2, pp. 818-824, February 2005.

[4] N. Budko and A. Samokhin, "Spectrum of the volume integral operator of electromagnetic scattering," *SIAM Journal on Scientific Computing*, vol. 28, pp. 682-700, 2006.

[5] R. Adams, "Physical and analytical properties of a stabilized electric field integral equation," I*EEE Transactions on Antennas Propagation*, vol. 52, no. 2, pp. 362-372, February 2004.

[6] F. Andriulli, K. Cools, H. Bağci, F. Olyslager, A. Buffa, S. Christiansen, and E. Michielssen, "A multiplicative calderón preconditioner for the electric field integral equation," *IEEE Transactions on Antennas Propagation*, vol. 56, no. 8, pp. 2398-2412, August 2008.

[7] H. Bağci, F. Andriulli, K. Cools, F. Olyslager, and E. Michielssen, "A calderón multiplicative preconditioner for coupled surface-volume electric field integral equations," *IEEE Transactions on Antennas Propagation*, vol. 58, no. 8, pp. 2680-2690, August 2010.

[8] D. Z. Ding, S. F. Tao, and R. S. Chen, "Fast analysis of finite and curved frequency-selective surfaces using the VSIE with MLFMA," *International Journal of Numerical Modeling: Electronic Networks, Devices and Fields*, vol. 5, pp. 425-436, 2011.

[9] M. Li, C. C. Lu, and Z. Zeng, "Localized preconditioning for radiation calculation of antennas mounted on large and complex platforms," *IEEE Antennas and Propagation Society International Symposium*, pp. 1899-1902, 2006.

[10] Y. Zhang, D. Huang, and J. Chen, "Combination of asymptotic phase basis functions and matrix interpolation method for fast analysis of monostatic RCS," *Applied Computational Electromagnetics Society (ACES) Journal*, vol. 28, no. 1, pp. 49-56, January 2013.

[11] O. Wiedenmann and T. Eibert, "Near-zone preconditioning investigations for integral equation solutions by method of moments," *28th Annual Review of Progress in Applied Computational Electromagnetics (ACES)*, Columbus, Ohio, pp. 1-6, April 2012.

[12] Z. N. Jiang, R. S. Chen, Z. H. Fan, Y. Y. An, M. M. Zhu, and K. W. Leung, "Modified adaptive cross approximation algorithm for analysis of electromagnetic problems," *Applied Computational Electromagnetics Society (ACES) Journal*, vol. 26, no. 2, pp. 160-169, February 2011.

[13] Z. N. Jiang, Z. H. Fan, D. Z. Ding, R. S. Chen, and K. W. Leung, "Preconditioned MDA-SVD-MLFMA for analysis of multi-scale problems," *Applied Computational Electromagnetics Society (ACES) Journal*, vol. 25, no. 11, pp. 914-925, November 2010.

[14] M. Li, M. Chen, W. Zhuang, Z. Fan, and R. Chen, "Parallel SAI preconditioned adaptive integral method for analysis of large planar microstrip antennas," *Applied Computational Electromagnetics Society (ACES) Journal*, vol. 25, no. 11, pp. 926-935, November 2010.

[15] J. F. Lee and D. K. Sun, "P-type multiplicative schwarz (pMUS) method with vector finite elements for modeling three-dimensional waveguide discontinuities," *IEEE Transactions on Microwave Theory and Technology*, vol. 52, no. 3, pp. 864-870, March 2004.

[16] J. F. Lee, R. Lee, and F. Teixeira, "Hierarchical vector finite elements with p-type non-overlapping schwarz method for modeling waveguide discontinuities," *CEMS-Computer Modeling in Engineering & Sciences*, vol. 5, no. 5, pp. 423-434, May 2004.

[17] T. Malas and L. Gurel, "Schur complement preconditioners for surface integral equation formulation of dielectric problems solved with the multilevel fast multipole algorithm," *SIAM Journal on Scientific Computing*, vol. 33, no. 5, pp. 2440-2467, May 2011.

[18] J. H. Yeom, H. Chin, H. T. Kim, and K. T. Kim, "Block matrix preconditioner method for the

electric field integral equation (EFIE) formulation based on loop-star basis functions," *Progress In Electromagnetic Research*, vol. 127, pp. 259-275, 2012.
[19] Y. Saad, "Iterative methods for sparse linear systems," 2nd Edition, *PWS*, 2003.
[20] W. C. Chew, J. M. Jin, E. Midielssen, and J. M. Song, "Fast and efficient algorithms in computational electromagnetics," *Artech House*, Boston, 2001.
[21] Y. L. Kolotilina, "Explicit preconditioning of systems of linear algebraic equations with dense matrices," *Journal of Soviet Mathematics*, vol. 43, no. 4, pp. 2556-2573, April 1988.
[22] N. Yuan, T. S. Yeo, X. C. Nie, L. W. Li, and Y. B. Gan, "Efficient analysis of electromagnetic scattering and radiation from patches on finite, arbitrarily curved, grounded substrates," *Radio Science*, vol. 39, 2004.

Shifei Tao was born in Anhui Province, China, in 1987. He received his B.S. degree in Communication Engineering from Nanjing University of Science and Technology (NUST), Nanjing, China, in 2008. He is currently working towards his Ph.D. degree at NUST. His current research interests include antennas, electromagnetic scattering and propagation.